

2.4. Intercomparison of products for climate applications

Hirohiko Masunaga¹, Fumie F. Akimoto¹, Takuji Kubota², Chris Kummerow³ and Marc Schröder⁴

¹ Institute for Space-Earth Environmental Research, Nagoya University, Nagoya, Japan

² Earth Observation Research Center, Japan Aerospace Exploration Agency, Tsukuba, Japan

³ Department of Atmospheric Science, Colorado State University, Fort Collins, CO, USA

⁴ Satellite-Based Climate Monitoring, Deutscher Wetterdienst, Offenbach, Germany

2.4.1. Introduction

Observational datasets of global precipitation are widely used for a range of climate applications, including atmospheric water and energy budget analyses (section 2.1) and climate model assessment (section 2.3), as well as meteorological studies on regional scales (for example, extreme events, see section 2.5) and synoptic scales (for example, tropical disturbances such as MJO). The precipitation products, however, are not strictly a “true” representation of nature but have their own uncertainties related to issues such as sampling errors and algorithmic assumptions. Extensive efforts have been made to document the biases in existing precipitation products. Such studies include the systematic assessment of numerous products on a global scale (for example, Gruber and Levizzani, 2008; Gehne et al., 2016; Beck et al., 2017; Sun et al., 2018) as well as a large body of literature on regional (typically continental-scale) intercomparisons (see review by Maggioni et al., 2016).

This assessment report is a concise update to existing efforts on the assessment of global precipitation products. Particular attention is paid to the potential bias characteristics in geographical pattern, ocean-land contrasts and mean versus extreme precipitation.

2.4.2. Data

In this sub-chapter, we analyze 11 global products consisting of the Climate Hazards Group InfraRed Precipitation with Station version 2 (CHIRPS v2.0, Funk et al., 2015), CMORPH v1.0 (Joyce et al., 2004; Xie et al., 2017), CPC v1.0 (Xie et al., 2007), GPCP Full Data Daily v2018 (Becker et al., 2013; Ziese et al., 2018), GPCP v1.3 daily (Huffman et al., 2001), GSMaP v6 (Kubota et al., 2007, 2020), Hamburg Ocean Atmosphere Parameters and Fluxes from Satellite Data (HOAPS) v4.0 (Andersson et al., 2010), IMERG v5 (Huffman et al., 2015, 2020), PERSIANN-CDR v1r1 (Ashouri et al., 2015), the Tropical Amount of Rainfall with Estimation of ERors (TAPEER) v1.5 (Roca et al., 2018), and TRMM Precipitation L3 1 day 0.25 degree x 0.25 degree V7 (TRMM 3B42 V7; Huffman et al., 2007). Note that HOAPS is an over-ocean product and the CHIRPS, CPC and GPCP data are available only over land. All estimates are adjusted to a daily 1°x1° grid in accordance with the FROGS data format (Roca et al., 2019). The analysis shown here is largely based on the results recently published by Masunaga et al. (2019).

Among these products, CMORPH, GPCP, GSMaP, IMERG, TAPEER and TRMM 3B42 all rely on the Low Earth Orbit (LEO) microwave radiometry and/or sounding data for baseline estimates of precipitation, with the GEO infrared measurements incorporated to fill in spatial and temporal gaps (see Section 1.1 for extended discussion on the methodology and error characterizations). In GPCP, GSMaP, IMERG and 3B42, a further adjustment is made with in situ measurements from gauge networks over land. See the individual documents cited above for product-specific details in the algorithmic strategy.

2.4.3. Results

Figure 2.4.1 shows the global (60°S-60°N) mean precipitation for different products with the daily data aggregated over 20 years from 1998 to 2017. The oceanic mean precipitation ranges from 2.39 mm/d to 3.4 mm/d, and the land mean precipitation varies between 1.81 mm/d and 2.28 mm/d. Note that the two gauge-only products (CPC and GPCC) largely disagree against each other, suggesting that uncertainties specific to gauge measurements such as sampling errors and the wind-induced undercatch may be as much responsible for the inter-product discrepancies as retrieval uncertainties in satellite algorithms (see section 1.2 for additional discussion on the utility and limitations of gauge measurements). This discrepancy partially accounts for the spread over land in the merged products as well, since IMERG is adjusted to GPCC over land and the daily GPCP is calibrated with GPCC through the monthly GPCP, while GSMaP and CMORPH adopt CPC for the gauge correction.

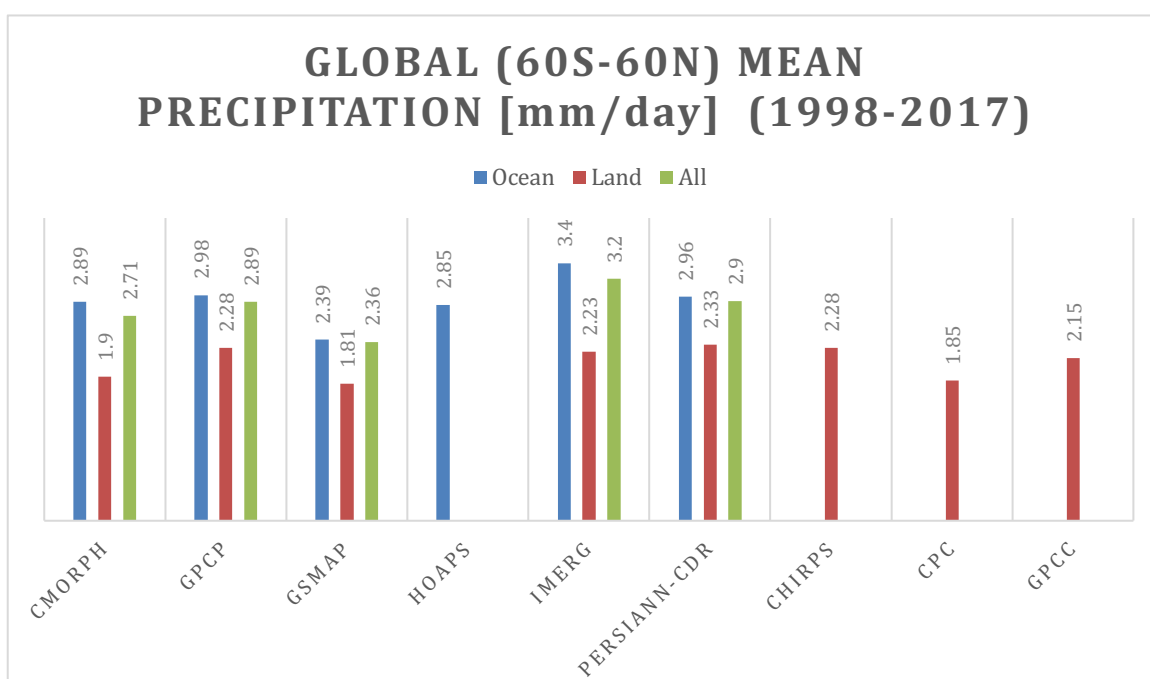


Figure 2.4.1. Global mean precipitation (mm/d) for each product (60°S-60°N, 1998–2017) over ocean (blue), land (orange) and all surfaces (gray). TAPEER and TRMM 3B42 are not included because these datasets do not cover the whole 60°S-60°N band.

Figure 2.4.2 presents the zonal-mean precipitation of different products for the year of 2015. All products qualitatively agree in the meridional structure of precipitation. A systematic bias, however, is evident in a quantitative sense, with the peak rainfall over ocean, representing the ITCZ, varying from 7 mm/d to 9 mm/d. The zonal-mean precipitation agrees better in the subtropics, but the spread expands over ocean for latitudes higher than 40°, where lighter precipitation that is difficult for radiometers to separate from cloud water, as well as some solid precipitation, makes the retrieval technically challenging (see also section 3.1). GSMaP marks the lowest while IMERG hits the highest at high latitudes as found in the global mean precipitation (Figure 2.4.1), while this order is reversed in the tropics. The uncertainty at high latitudes is a primary driver of the inter-product spread in the global-mean precipitation. Precipitation over land in the northern high latitudes reasonably agrees among different products, presumably owing to the dense gauge networks there to which satellite estimates are adjusted.

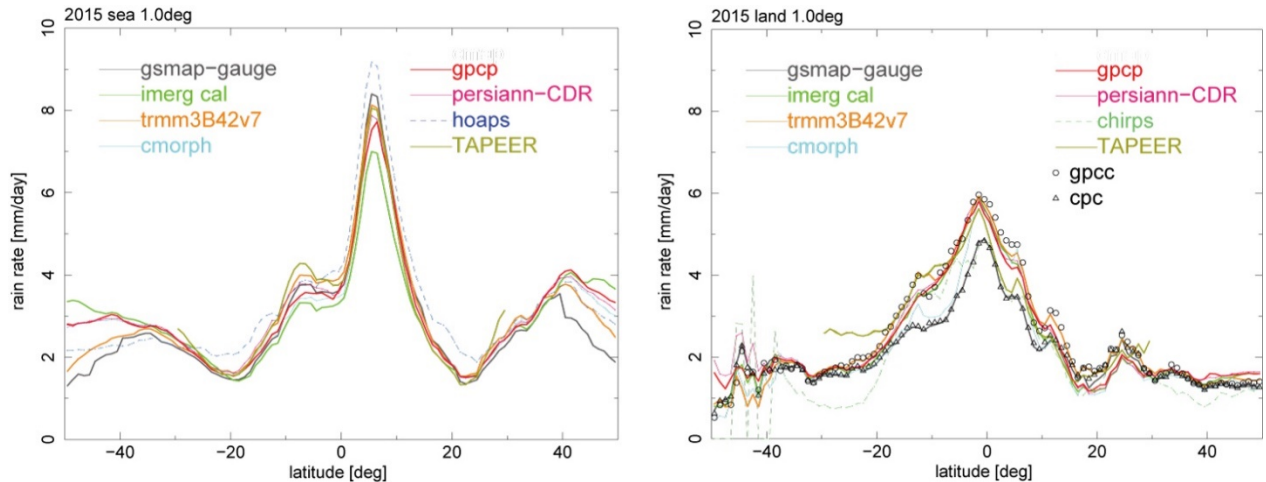


Figure 2.4.2. Zonal mean precipitation (mm/d) over ocean (left) and over land (right) for the year of 2015. Adopted from Masunaga et al. (2019)

The global distribution of all the products averaged together and the anomalous geographical pattern for selected products from the ensemble mean is depicted in Figure 2.4.3. The GSMaP annual-mean precipitation is higher in the Pacific ITCZ and lower elsewhere than the ensemble mean, while the IMERG precipitation is just opposite in geographical pattern to GSMaP. This striking contrast is somewhat surprising, given that GSMaP and IMERG share aspects of the fundamental product design such as the native grid resolution (0.5°), temporal sampling (hourly for GSMaP and half-hourly for IMERG), and the overall algorithmic flow (LEO microwave → GEO infrared morphing → gauge adjustment). When compared in extreme (ninety-ninth percentile) precipitation, GSMaP and IMERG, however, have fundamentally different anomaly patterns relative to their annual means. Both the two products stay lower than the ensemble mean across global oceans, while the anomaly is opposite in sign over land. This particular case offers an illustrative example that the bias characteristics in the climatological precipitation are generally a poor predictor of the extreme rain biases. See Masunaga et al. (2019) for the global maps of the other products included in the assessment.

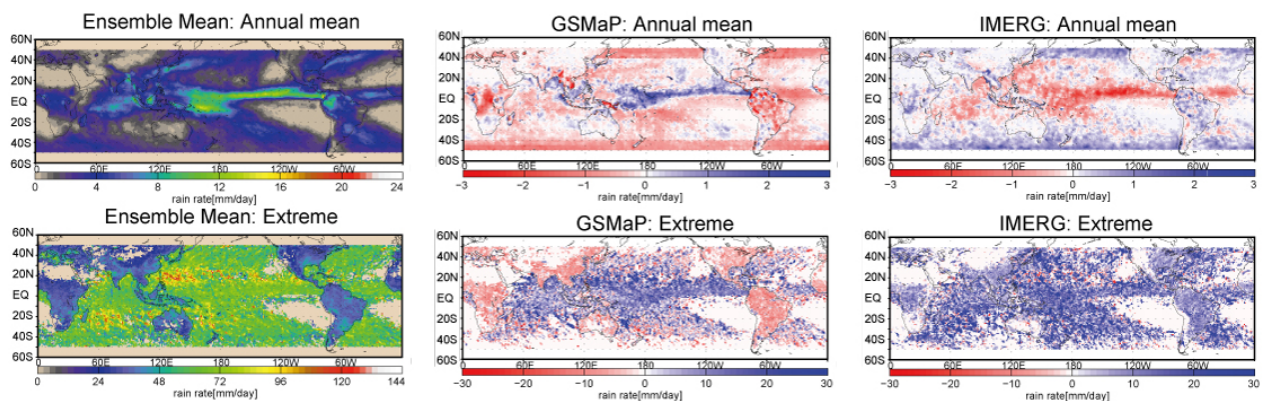


Figure 2.4.3. Global map of annual-mean precipitation (top) and ninety-ninth percentile extreme precipitation or R99p (bottom) for the year of 2015. The ensemble mean of all products (left) and the anomaly from the ensemble mean for selected products: GSMaP (middle) and IMERG (right). Adopted from Masunaga et al. (2019)

Finally, the deseasonalized time series of different products are shown in Figure 2.4.4. Different curves are found to be clustered into a few groups rather than spread widely. The monthly-mean precipitation agrees relatively well over oceans with the exception of GSMaP, staying somewhat lower. Some products exhibit more pronounced interannual variability than others: HOAPS has a striking peak associated with the 1997 El Niño, and PERSIANN shows a sharp minimum of unknown origin in 2017. Over land, the monthly-mean precipitation appears to be divided into two groups anchored to the two-gauge products (GPCC and CPC). This may be partly due to the gauge adjustment procedure carried out in each product. The ninety-ninth percentile extremes are spread more widely than the monthly mean. Oceanic extremes in GPCP and PERSIANN, the latter of which is adjusted to the former in monthly mean, are modest in intensity relative to other datasets. As such, the bias characteristics specific to each product are essentially different between the mean and extreme precipitation as noted above.

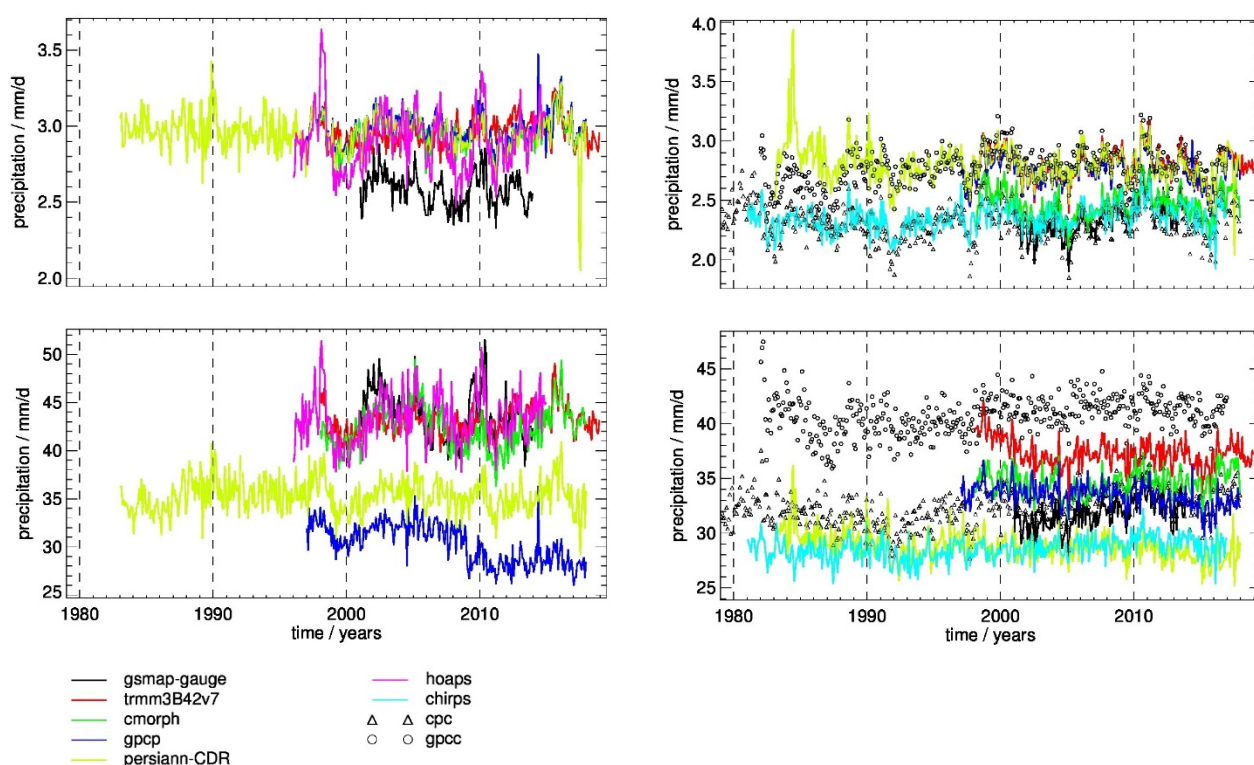


Figure 2.4.4. Time series of monthly mean precipitation with the annual cycle being removed: global ocean (left column) and global land within 50°N/S (right column), mean over all defined values (top row), and ninety-ninth percentile (bottom row). Adopted from Masunaga et al. (2019)

2.4.4. Fitness of gridded daily observations for different applications

Spatial and temporal resolutions and the period of data record depend largely on the products. Those with fine grid intervals include CHIRPS (0.05°) and GSMaP and IMERG (0.1°). The temporal sampling is as dense as half-hourly for IMERG and hourly for GSMaP. The data record dates back to the late nineteenth century for a monthly version of GPCC, but is otherwise limited to more recent decades. Most satellite-based products are available only after late 1990s with a few exceptions, including the monthly GPCP, which is available for 1979 onwards. The products with fine resolutions may be of great utility for regional hazard monitoring, while those with decades of data record would be optimal for climate studies focused on long-term changes in the water cycle. It is noted that a grid size as small as 0.1°

does not necessarily guarantee that the information content is as fine as 10 km, since low-frequency microwave FOVs are significantly larger than 10 km.

Among the critical requirements for operational applications is data latency. Many of the products (CMORPH, GSMaP, IMERG, and PERSIANN, for instance) offer a near-real-time option in which the data are distributed to the users as quickly as possible at the expense of accuracy (for example, Kubota et al., 2020). The same products often provide a better calibrated version at a later time for general users who prioritize reliability over latency.

This assessment is not intended to show which product is “better” than another because the absolute reference does not exist. One of the primary goals of the assessment is to document the characteristics of structural bias in hopes to help the dataset providers further refine the algorithm. The intercomparison results shown above would change as the participating products are upgraded to future versions. The assessment will need to be regularly updated as well to accommodate the continuous evolution of the products.

2.4.5. Summary

We presented in this sub-chapter an intercomparison of 11 global precipitation datasets. Major conclusions are:

- i. While the overall geographical pattern of precipitation is coherent among products, the magnitude varies from one dataset to the other. The agreement is poor particularly at high latitudes, since light and/or solid precipitation typical of high latitudes is difficult to estimate accurately from satellite microwave radiometry.
- ii. A systematic bias is present between gridded gauge products (GPCC and CPC), which is presumably partially responsible for the spread in merged multi-satellite datasets adjusted to the gauge products.
- iii. The bias characteristics in the annual/monthly mean precipitation are a poor predictor of those in extreme precipitation.

2.4.6. Recommendations

Specific recommendations to this chapter are:

- i. An accurate estimation of the tropical precipitation is important as an observational constraint on the tropical dynamics (Hadley cells, MJO, etc.) and the Earth energy budget. The current uncertainty in the ITCZ rainfall (7 mm/d–9 mm/d) could be problematic and further effort is urged to reconcile this discrepancy.
- ii. The inter-product spread is large at latitudes higher than 40°S/N. This high-latitude uncertainty is among the major factors responsible for the disagreement in the global-mean precipitation. To mitigate this issue, further improvement is critically important on the estimation of cold-season precipitation. The difficulty in separating cloud water from light rainfall is likely another source of uncertainty in the microwave retrieval of precipitation and requires better modeling in the algorithm.
- iii. Many products apply a gauge adjustment to satellite-based precipitation estimates over land. The present intercomparison reveals that the uncertainties intrinsic of gridded gauge datasets (GPCC and CPC) can be a bottleneck for all the products internally using these data as a reference. Better consistency between different gauge products is critically desired.

- iv. Uncertainties in accumulations have not been reduced significantly from many regional validation studies. More emphasis on physically derived uncertainties for weather and climate applications will be critical to gain confidence in these products going forward.

2.4.7. References

Andersson, A., K. Fennig, C. Klepp, S. Bakan, H. Grassl and J. Schulz, 2010: The Hamburg Ocean Atmosphere Parameters and Fluxes from Satellite Data - HOAPS-3. *Earth System Science Data*, **2**, 215–234.

Ashouri, H., K.-L. Hsu, S. Sorooshian, D.K. Braithwaite, K.R. Knapp, L.D. Cecil, B.R. Nelson and O.P. Prat, 2015: PERSIANN-CDR: Daily precipitation climate data record from multi-satellite observations for hydrological and climate studies. *Bulletin of the American Meteorological Society*, **96**, 69–83.

Beck, H.E., N. Vergopolan, M. Pan, V. Levizzani, A.I.J.M. Van Dijk, G.P. Weedon, L. Brocca, F. Pappenberger, G.J. Huffman and E.F. Wood, 2017: Global-scale evaluation of 22 precipitation datasets using gauge observations and hydrological modeling. *Hydrology and Earth System Sciences*, **21**(12), 6201–6217, doi:10.5194/hess-21-6201-2017.

Becker, A., P. Finger, A. Meyer-Christoffer, B. Rudolf, K. Schamm, U. Schneider and M. Ziese, 2013: A description of the global land-surface precipitation data products of the Global Precipitation Climatology Centre with sample applications including centennial (trend) analysis from 1901–present. *Earth System Science Data*, **5**, 71–99.

Funk, C., P. Peterson, M. Landsfeld, D. Pedreros, J. Verdin, S. Shukla, G. Husak, J. Rowland, L. Harrison, A. Hoell and J. Michaelsen, 2015: The climate hazards infrared precipitation with stations—A new environmental record for monitoring extremes. *Scientific Data*, **2**, 1–21.

Gehne, M., T.M. Hamill, G.N. Kiladis and K.E. Trenberth, 2016: Comparison of global precipitation estimates across a range of temporal and spatial scales. *Journal of Climate*, **29**, 7773–7795.

Gruber, A., and V. Levizzani (eds.), 2008: *Assessment of global precipitation products*. WCRP Series Report No. 128 and WMO TD-no. 1430, Geneva.

Huffman, G.J., R.F. Adler, M.M. Morrissey, D.T. Bolvin, S. Curtis, R. Joyce, B. McGavock and J. Susskind, 2001: Global Precipitation at One-Degree Daily Resolution from Multisatellite Observations, *Journal of Hydrometeorology*, **2**, 36–50.

Huffman, G.J., R.F. Adler, D.T. Bolvin, G. Gu, E.J. Nelkin, K.P. Bowman, Y. Hong, E.F. Stocker and D.B. Wolff, 2007: The TRMM Multi-satellite Precipitation Analysis: Quasi-global, multi-year, combined-sensor precipitation estimates at fine scale. *Journal of Hydrometeorology*, **8**, 38–55.

Huffman, G.J., D.T. Bolvin and E.J. Nelkin, 2015: *Day 1 IMERG Final Run Release Notes*. https://gpm.nasa.gov/sites/default/files/document_files/IMERG_FinalRun_Day1_release_notes.pdf.

Huffman, G.J., D.T. Bolvin, D. Braithwaite, K.-L. Hsu, R.J. Joyce, C. Kidd, E. J. Nelkin, S. Sorooshian, E.F. Stocker, J. Tan, D.B. Wolff and P. Xie, 2020: Integrated Multi-satellite Retrievals for the Global Precipitation Measurement (GPM) Mission (IMERG). In: *Satellite Precipitation Measurement* (V. Levizzani, C. Kidd., D.B. Kirschbaum, C.D. Kummerow, K.

Nakamura, F.J. Turk, eds.). Springer Nature, Cham, *Advances in Global Change Research*, 67, 343–353, https://doi.org/10.1007/978-3-030-24568-9_19.

Joyce, R.J., J.E. Janowiak, P.A. Arkin and P. Xie, 2004: CMORPH: A Method that Produces Global Precipitation Estimates from Passive Microwave and Infrared Data at High Spatial and Temporal Resolution. *Journal of Hydrometeorology*, 5, 487–503.

Kubota, T., S. Shige, H. Hashizume, A. Aonashi, N. Takahashi, S. Seto, M. Hirose, Y.N. Takayabu, T. Ushio, K. Nakagawa, K. Iwanami, M. Kachi and K. Okamoto, 2007: Global Precipitation Map Using Satellite-Borne Microwave Radiometers by the GSMaP Project: Production and Validation. *IEEE Transactions on Geoscience and Remote Sensing*, 45, 2259–2275.

Kubota, T., K. Aonashi, T. Ushio, S. Shige, Y.N. Takayabu, M. Kachi, Y. Arai, T. Tashima, T. Masaki, N. Kawamoto, T. Mega, M.K. Yamamoto, A. Hamada, M. Yamaji, G. Liu and R. Oki, 2020: Global Satellite Mapping of Precipitation (GSMaP) products in the GPM era. In: *Satellite Precipitation Measurement* (V. Levizzani, C. Kidd., D. B. Kirschbaum, C. D. Kummerow, K. Nakamura, F.J. Turk, eds.), Springer Nature, Cham, *Advances in Global Change Research*, 67, 355–373, https://doi.org/10.1007/978-3-030-24568-9_20.

Maggioni, V., P. Meyers and M. Robinson, 2016: A review of merged high resolution satellite precipitation product accuracy during the Tropical Rainfall Measuring Mission (TRMM)-Era. *Journal of Hydrometeorology*, 17, 1101–1117.

Masunaga, H., M. Schröder, F.A. Furuzawa, C. Kummerow, E. Rustemeier and U. Schneider, 2019: Inter-product biases in global precipitation extremes. *Environmental Research Letters*, 14, 125016, doi:10.1088/1748-9326/ab5da9.

Roca, R., N. Taburet, E. Lorant, P. Chambon, M. Alcoba, H. Brogniez, S. Cloché, C. Dufour, M. Gosset and C. Guilloteau, 2018: Quantifying the contribution of the Megha-Tropiques mission to the estimation of daily accumulated rainfall in the Tropics. *Quarterly Journal of the Royal Meteorological Society*, 144 (Suppl. 1), 49–63.

Roca, R., L.V. Alexander, G. Potter, M. Bador, R. Jucá, S. Contractor, M.G. Bosilovich and S. Cloché, 2019: FROGS: a daily 1° × 1° gridded precipitation database of rain gauge, satellite and reanalysis products. *Earth System Science Data*, 11, 1017–1035, <https://doi.org/10.5194/essd-11-1017-2019>.

Sun, Q., C. Miao, Q. Duan, H. Ashouri, S. Sorooshian and K.L. Hsu, 2018: A Review of Global Precipitation Data Sets: Data Sources, Estimation, and Intercomparisons. *Reviews of Geophysics*, 56(1), 79–107, doi:10.1002/2017RG000574.

Xie, P., A. Yatagai, M. Chen, T. Hayasaka, Y. Fukushima, C. Liu and S. Yang, 2007: A gauge-based analysis of daily precipitation over East Asia. *Journal of Hydrometeorology*, 8, 607–626.

Xie, P., R. Joyce, S. Wu, S. Yoo, Y. Yarosh, F. Sun and R. Lin, 2017: Reprocessed, Bias-Corrected CMORPH Global High-Resolution Precipitation Estimates from 1998. *Journal of Hydrometeorology*, 18, 1617–1641.

Ziese, M., A. Rauthe-Schöch, A. Becker, P. Finger, A. Meyer-Christoffer and U. Schneider, 2018: GPCC Full Data Daily Version 2018 at 1.0°: Daily Land-Surface Precipitation from Rain-Gauges built on GTS-based and Historic Data. DOI: 10.5676/DWD_GPCC/FD_D_V2018_100.